Creep Behaviour of Aluminium 7075 Feedstock Billet Globular Microstructure at High Processing Temperature

A. Megalingam[a], A.H. Ahmad[a,b,] *, N.A. Alang[a], J. Alias[a], S. Naher[c]

[a] Faculty of Mechanical and Automotive Engineering Technology,
Universiti Malaysia Pahang Al-Sultan Abdullah, 26600 Pekan, Pahang, Malaysia.

[b] Advanced Industrial Technology Research Center,
Universiti Malaysia Pahang Al-Sultan Abdullah, 26600 Pekan, Pahang, Malaysia.

[c]Department of Mechanical Engineering and Aeronautics, City
University of London, London EC1V 0HB, UK.

**asnul@umpsa.edu.my*

Abstract:

This paper aims to present the determination of the creep behaviour of a globular microstructure aluminium 7075 alloy semisolid metal feedstock billets under a constant temperature of 250 °C. Globular microstructures are often preferred in thixoforming processes due to their unique properties, and favourable mechanical and high-temperature applications. Less attention has been given to globular microstructure even though the contribution of microstructure to creep behaviour is essential. Therefore, for this test,

- Globular microstructure aluminium 7075 alloy feedstock billets were produced by the Direct Thermal Method (DTM).
- The creep tests were conducted at different stress ranges from 30 to 70 MPa, and the effect of globular microstructure was examined.
- The results showed that the globular microstructure had the least deformation and the lowest creep rate at a longer deformation time.
- The fracture surface of the samples was then analysed with scanning electron microscopy (SEM). The microstructural changes that occurred during the test were investigated.

SEM analysis revealed that the globular microstructure of the feedstock billet exhibits fewer voids and defects due to a uniform microstructure. The strain exponent value of globular microstructure billets was found to be at n= 4.6 in the stress range between 30 to 70 MPa at a constant temperature. This study is expected to provide an understanding of the creep behaviour of globular microstructures at high temperatures and high-stress conditions.

Keywords: Aluminium 7075 alloy, Globular microstructure, Feedstock billets, Creep behaviour, Creep strain, Strain exponent.

1. Introduction

Aluminium alloys are used in various applications from aerospace components to automotive components and beyond due to their lightweight and superplastic nature [1]. It is in high demand in nuclear reactor components such as heat exchangers, coated electrical conductors, cladding materials, radiation shielding materials, and nuclear fuel shields [2–4]. However, several studies point out the problems in casting these alloys such as the mechanical properties of aluminium alloys in high-temperature applications [5]. Although the high silicon content in aluminium alloys is advantageous in casting, it also increases brittleness, making the material prone to cracking and fracture. Previous studies have reported that aluminium 7075 alloy with low silicon content has better mechanical properties than other aluminium grades, however, there are problems with casting low-silicon alloys [6,7]. Semi-solid metal (SSM) processing offers several advantages over conventional metal casting methods [8]. There is evidence that the globular microstructure has provided various technological advantages in the SSMP process with emphasis on microstructure [9]. Generally, the grain size of aluminium alloys is 100 to 500 μm or larger, depending on the liquid metal temperature and cooling rate. Aluminium alloys with grain sizes less than 100 μm are for high-strength applications. A grain size of 50 to 100 μm is preferred for globular microstructure for better flow behaviour and fewer defects [10]. DTM method is known as a simple and low-cost method to produce globular microstructures [11]. This kind of research is necessary to produce high-quality products in a semi-solid process such as thixo forming and to understand the behaviour of globular microstructure aluminium 7075 alloy billets. Further attention is needed to understand the stability and performance of globular microstructure billets for long-term use.

Microstructure plays a major role in improving physical properties in aluminium 7075 alloys, particularly in the induction of secondary growth required for high-rate and high-temperature deformation when using grain-refined alloys [12]. Non-dendritic globular microstructures excel in the thixoforming process with superior mechanical properties [13]. However, explanations about globular microstructure formation and parameters are lacking. Investigation of creep behaviour is necessary to indicate the time-dependent deformation or strain that occurs when a material is subjected to constant temperature and stress. [14–16]. The creep behaviour of metals at high temperatures has always been a matter of debate. Furthermore, it is of interest to investigate the creep behaviour of aluminium alloys preferred for SSM process applications along with microstructural effects. AZ81 Mg samples with uniform microstructure were found to provide significant creep resistance in high cyclic fatigue tests performed at temperatures from 423 to 523 K in the stress range of 200 to 700 MPa [17]. Fine microstructures were also observed in magnesium alloys that provided high tensile strength [18]. Tensile strength may be reduced due to porosity and casting defects in the uneven microstructure commonly found in cast materials, however, materials with uniform small particles prepared for thixoforming may provide good tensile strength. In terms of creep behaviour, alloys with coarser microstructures generally have higher creep resistance compared to alloys with fine microstructures.

The 2xxx, 6xxx, and 7xxx series of aluminium alloys are commonly used for high-temperature applications. Aluminium 7xxx series is suitable for high hardness heat treatment, contains Zn as the main alloying element and has an ultimate tensile strength range value from 32-

88ksi. It has a yield strength of 455 MPa and a low density (2.81 g/cm^3), allowing the composite to retain its strength at elevated temperatures and contributing to its exceptional strength-to-weight ratio. Aluminium 7075 alloy had a strain rate range of 0.001 to 0.05 s^{-1} in the temperature range of 623 to 723 K under constant stress [19]. Semi-solid casting 7075-T6 composites prepared by gas induction showed a good response when subjected to creep deformation behaviour [20]. Less research has been done on the creep behaviour of cast materials required for SSM processes such as thixoforming, especially with microstructure implications. Therefore, a thorough investigation of the creep deformation of globular microstructure aluminium 7075 alloy billet is important to predict its long-term behaviour and to confirm the structural stability of the component subjected to prolonged loading. Understanding and controlling creep behaviour is essential to ensure the structural integrity and reliability of components subjected to prolonged loading at elevated temperatures and stresses that describe the relationship between strain rate and stress in the creep regime [21].

Creep behaviour has been extensively studied in various aluminium alloys series with less attention has been given to high-strength aluminium 7075 alloys [14,22]. Numerous investigations demonstrated that the creep resistance of aluminium alloys is significantly influenced by their microstructure. However, there is a lack of information in the literature on the creep behaviour of globular microstructure especially produced by SSM processing. There is a research gap and necessity in the study of the creep behaviour of aluminium 7075 alloys globular microstructure [21,23,24]. Therefore, this novel study aims to investigate the creep behaviour of aluminium 7075 alloys globular microstructure billets under different stress conditions at a constant temperature of 250 °C. The results of this study are expected to provide an understanding of the creep behaviour of aluminium 7075 globular microstructure for high-temperature and high-stress applications.

2. Experimental Procedures

2.1 Material

The chemical composition of aluminium 7075 alloys used in this study was analyzed by Optical Emission Spectroscopy (OES), Foundry Master Oxford Instruments (FMOI). The findings of the investigation are displayed in Table 1.

Table 1 Chemical composition of aluminium 7075 alloy.

Element wt%								
Al	**Mg**	**Cu**	**Zn**	**Fe**	**Cr**	**Mn**	**Si**	**Ti**
89.7	2.24	1.46	5.8	0.17	0.22	0.04	0.12	0.04

2.2 Globular Structure Feedstock Billet Preparation

The Direct Thermal Method (DTM) has proven to be a cost-effective way to produce aluminium 7075 alloy feedstock billets for the SSM process and offers many advantages such as reduced production time, simplicity, and high quality. Aluminium 7075 alloy has a melting

temperature of 635 °C, however, previous study results have defined a pouring temperature of 665 °C and a holding time of 60 s to produce aluminium 7075 alloy feedstock billet with fine and globular microstructure by the DTM method [11,25]. This study followed these parameters. A K-type thermocouple was used to measure the temperature of the molten liquid. The molten liquid was poured into a cylindrical copper mould of 130 mm height, 25 mm diameter, and 1 mm thickness at a temperature of 665 °C. After a 60 s holding time, the mould was quenched in the room-temperature water.

2.3 Creep Experiment

The creep test, also known as the constant load, constant temperature test, is a method used to determine the creep behaviour of materials. A Creep test has been used in this study to investigate the creep deformation behaviour of globular microstructure aluminium 7075 alloy feedstock billets. It involves applying a constant load to a specimen at a constant temperature and measuring the deformation over time. The process of conducting this creep test involves several steps. The specimen was prepared in aluminium 7075 alloy metal in the shape of a dumbbell with the dimensions shown in Fig. 1. According to ASTM E139-11(2018), the cylindrical specimen has a gauge length of 36 mm and a diameter of 8 mm [26].

Fig. 1. Creep specimen photo view.

The specimen was mounted in a creep testing machine and subjected to a static load of 30 to 70 MPa at a constant temperature (250 °C). The temperature was monitored by K-type-thermocouples attached to the center, edges of the specimen. A pair of LVDT sensors is attached to the sample to measure the deformation of the sample. The creep experimental setup photo view is presented in Fig. 2. During the test, the sample was kept at an isothermally for an hour to remove the thermal gradient before the load was applied, which is known as the pre-loading process. It helped to remove residual stresses present in the specimen. The heating system and loading stress have 1 K and 0.1 MPa precisions, respectively. A computer with a data logger was used to automatically manipulate, control, and collect data from experimental procedures.

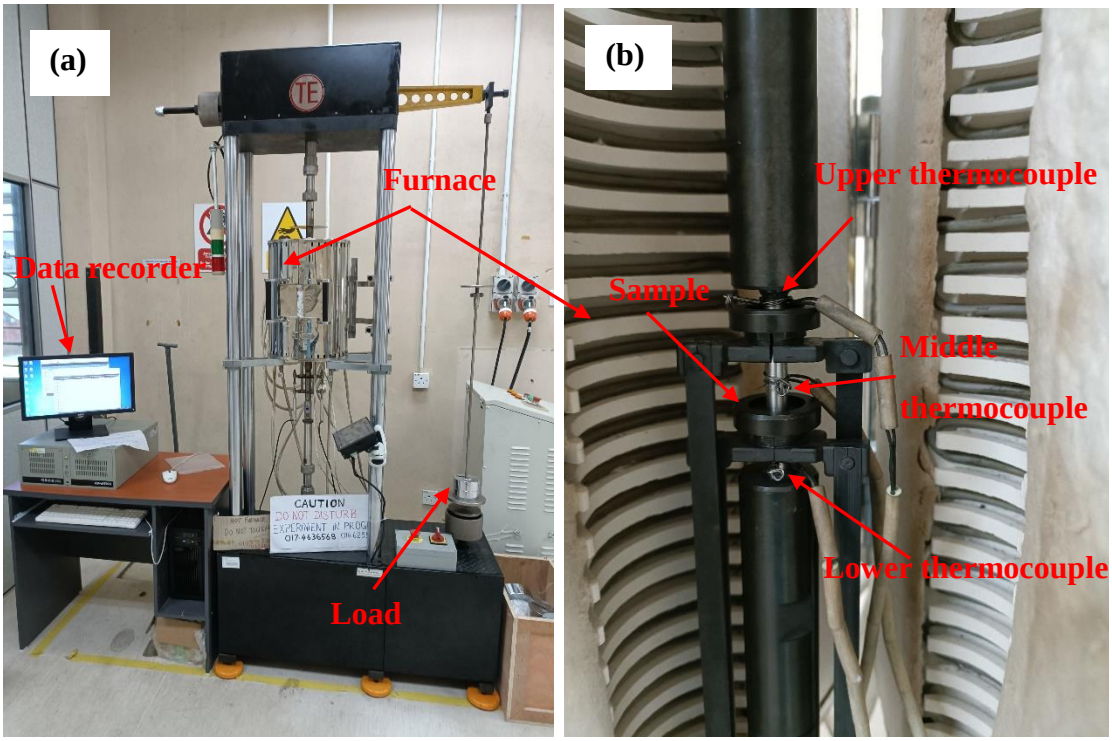

Fig. 2. (a) Creep machine photo view, and (b) Zoomed view of sample with inside of the furnace.

In the context of creep testing, the temperature and microstructure-dependent constant is typically represented by the Norton-Bailey equation, also known as the power law creep equation. It relates the creep rate ($\dot{\varepsilon}$) to the applied stress (σ), temperature (T), and material-dependent parameters. The general form of the Norton-Bailey Eq. (1) is as follows [23].

$$\text{Creep rate } (\dot{\varepsilon}) = \mathrm{A} * \sigma^{n} * \exp(-\frac{Q}{RT}) \qquad (1)$$

Where έ = creep rate (strain per unit time), A = material constant, σ = Applied stress, n = stress exponent, Q = activation energy for creep, R = universal gas constant, T = absolute temperature. The power law Eq. (2) for creep is given by [23],

$$Creep\ strain\ (\varepsilon) = A * t^n \quad (2)$$

where ε = creep strain, t = time, A = constant, and n = strain exponent. On a log-log scale, this Eq. (3) becomes,

$$\log(\varepsilon) = \log(A) + \mathrm{n} * \log(\mathrm{t}) \quad (3)$$

The strain exponent in creep testing plays a crucial role in understanding and predicting the creep behaviour of materials. It aids in design, reliability assessment, material selection, and process optimization, ultimately leading to safer and more efficient engineering solutions. Understanding the strain exponent is crucial for designing components and structures that will be subjected to long-term or high temperature loading conditions. Moreover, this study describes the relationship between minimum creep rate and applied creep stress at constant temperature through Norton's law Eq. (4) [23].

$$Minimum\ creepstrain\ \varepsilon_{min} = A\sigma^n \quad (4)$$

where A = temperature-dependent material parameter, $\boldsymbol{\sigma}$ = stress applied on the sample, ε min = minimum creep strain rate, and n = stress exponent.

2.4 SEM Experiment

The Scanning Electron Microscope (SEM) was used to evaluate surface pictures of post-fracture specimens. The SEM analysis involved various steps. First, the sample to be measured for SEM analysis was carefully cut to 20 mm and prepared. The prepared creep fracture specimen was securely mounted on the SEM specimen stub using conductive adhesive. The sample stub was labelled to identify the sample name details. Then vacuum and electron gun initiation process was performed for SEM study. The SEM was switched on and heated to 25 °C according to the manufacturer's instructions, and the acceleration voltage was set to 30 kV. The SEM imaging method was used to detect the selected area in the creep fracture specimen. Low magnification was used for initial navigation. Then SEM images were obtained by adjusting the magnification step by step. Accurate images were obtained using magnifications ranging from 50 x to 500 x at different locations. An initial image of the entire fracture surface was captured at low magnification

to assess the overall morphology and identify specific areas. Magnification was gradually increased to focus on specific features such as cracks and voids. In this experiment, the SEM images of an aluminium 7075 alloy billet specimen tested at a constant temperature of 250 °C at a stress of 50 MPa and 70 MPa were examined. Also, the surfaces of the base material subjected to creep test under a stress of 50 MPa at the same constant temperature were also investigated. Fracture damage, microstructural changes, presence of voids or cracks, microstructural bonding, and fracture information were investigated.

3. Results and Discussion

3.1 Microstructure Analysis

The primary particle size and shape in the microstructure of the feedstock billet prepared at 665°C pouring temperature and 60 s holding time were examined. Fig. 3 displays the obtained microstructure images. The average grain diameter, circularity, and aspect ratio of primary phase particles of feedstock billet prepared with globular microstructure were 57.33 µm, 0.72, and 1.43, respectively. Previous studies have suggested that the desired globular microstructure in semisolid processing methods requires a particle grain size below 100 µm, a circularity close to 1, and a low aspect ratio. The microstructure of aluminium 7075 alloy feedstock billets obtained in this study had a large number of fine and uniform globular microstructures in good agreement with previous findings [11,25].

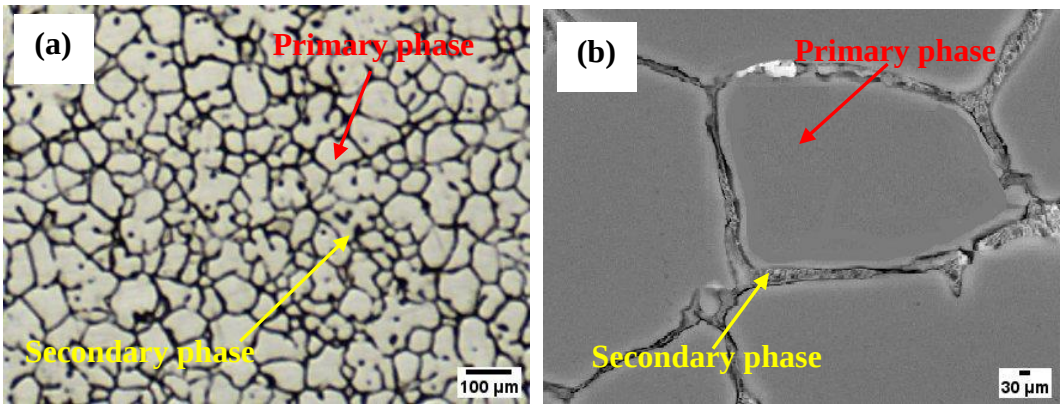

Fig. 3. Microstructure images of feedstock billet prepared using the DTM method at a pouring temperature of 665 °C and holding time of 60 s: (a) Lower magnification and (b) Higher magnification.

3.2 Creep Analysis

The creep behaviour of dendrite and globular microstructure materials was studied, and the obtained results are shown in Table 2.

Table 2: Correlation for maximum creep rate and creep stress of globular microstructure aluminium 7075alloy feed stock billet at 250 °C.

Sample number	Temperature (°C)	Material (AA7075)	Stress (MPa)	Max. Creep Strain	Rupture Time (hrs)
1	250	Billet	30	0.03	52.25
2	250	Billet	50	0.05	20.55
3	250	Billet	60	0.06	1.20
4	250	Billet	70	0.08	0.29
5	250	Original	50	0.18	34.35

The results show that the creep rupture time of aluminium 7075 alloy billets is lowest at 60 and 70 MPa stress and maximum at 50 MPa and 30 MPa. It shows that the billets responded well to creep deformation. A very short creep rupture time affects the primary and secondary creep

curves (Fig. 4). At 30 MPa stress, the creep deformation of the globular microstructure aluminium 7075 alloy feedstock billet was lower than in other samples. It indicates that this globular microstructure material is resistant to creep deformation at low-stress levels [4].

In this experiment, results show how an aluminium 7075 alloy feedstock billet with a globular microstructure responds to different stress. Compared to the original material with a coarser microstructure, it had a lower creep rate and took less time to reach the creep strain. However, it has well responded favourably when compared to the creep rate observed in structures prepared for previous semi-solid processing methods [24,25]. At low-stress levels, creep deformation, governed by diffusion process rather than dislocation motion, eventually led to plastic deformation. The creep strain time curves under temperature of 250 °C are shown in Fig. 4.

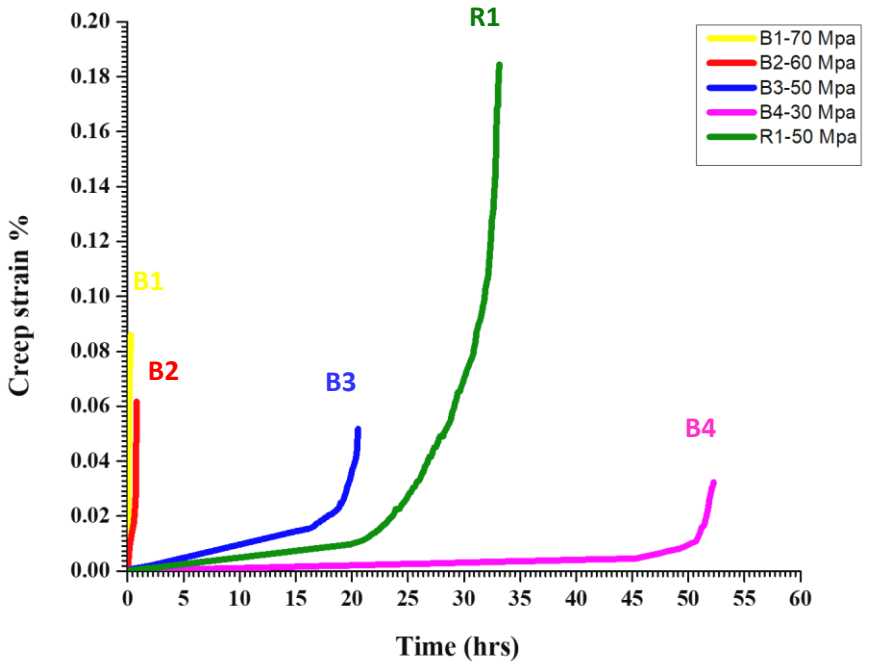

Fig. 4. Creep strain time curves under temperature of 250 °C.

The results of this study provide valuable information for the design of structures and components made from aluminium 7075 alloy. The resistance to grain boundary sliding, influenced by factors like grain size, grain boundary character, and grain boundary cohesion, contributes to the resistance against creep deformation. The observed creep behaviour suggests a distinction between dendrite and globular microstructures. The globular structure, with its larger grain size, is less likely to have defects such as voids and inclusions, which act as sites for creep deformation to initiate. Additionally, the larger grains provide greater resistance to deformation due to their lower curvature and higher elastic modulus. At 250 °C and 50 MPa stress, the creep behaviour of the original aluminium 7075 alloy and globular microstructure feedstock billet was studied. The results of the study show that the billet material creeps rapidly and breaks before

reaching the specified creep strain. However, the original material specimen (R1) had better resistance to creep until the higher strain value was reached. Aluminium 7075 alloys show good resistance with low creep value when compared to other aluminium and microstructures. Several studies have reported that the dendrite microstructure commonly found in the original material consists of elongated, tree-like crystal structures with a complex shape. In contrast, globular microstructures consist of uniformly sized spherical grains dispersed throughout the material [7],[28]. Coarse grains found in dendritic microstructures acted as stress concentration sites and dislocation motion without fracture. Globular microstructures typically consist of equilibrated grains that are less resistant to dislocation motion and grain boundary sliding but fracture soon. For example, a high-silicon aluminium alloy such as A 356 has a maximum creep strain value of 0.2 to 0.3%. Meanwhile, alloys such as low-silicon aluminium 7075 alloy have predicted maximum creep strain values of 0.1 to 0.2%. The results of this study are in good agreement with this [20,23,24]. Fine and uniform grain sizes inhibit the movement of dislocations that cause plastic deformation. Its grain boundaries and dislocation interactions with other dislocations create re-stresses that inhibit the movement of dislocations, thus preventing creep. The result of this study provides valuable information for the design of microstructures and components manufactured from aluminium 7075 alloy globular structured feedstock billets. It proved to be capable of withstanding high temperature and load conditions. Moreover, the findings of this study suggest the importance of microstructure in alloys also contributes to the prediction and development of creep behaviour.

3.3 SEM Analysis

Photographs of the fractured specimens after creep testing are presented in **Fig. 5**. The image of the fractured specimen provided valuable insights into the creep behaviour and changes in the specimen during failure.

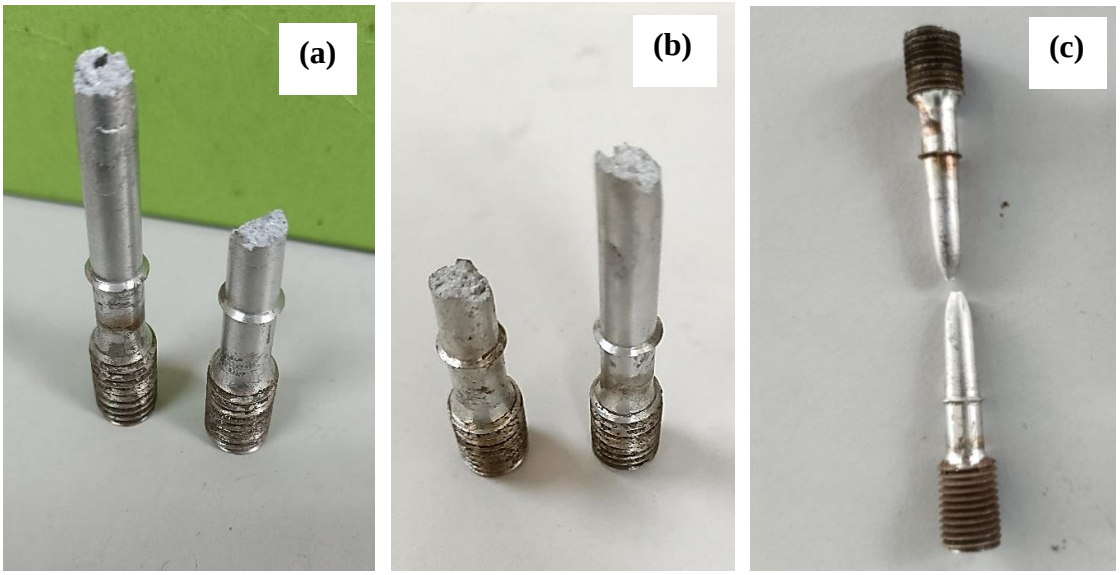

Fig. 5. Photographic images of fracture tested specimens presented: (a) 50 MPa (Globular microstructure billet), (b) 70 MPa (Globular microstructure Billet) and (c) 50MPa (Original material non-billeted).

The decreased cross-sectional area before fracture can be seen in specimen (c) of **Fig. *5***. The original (non-billeted) specimen has developed a neck before ultimate failure, showing that it has undergone significant plastic deformation. It was shown that the billet specimen exhibited uniform deformation behaviour but had a low tendency to necking. Small pits were observed on the surface of the fractured areas in the billet specimen. Furthermore, the billet samples deformed with less necking, and then fractured in a semi-split pattern as observed in the macroscopic sample. The original specimen appears to have very small cracks at the fracture region. Microscopic observations and creep cavities were investigated by SEM study to explain the causes of the formation of small microcracks. This SEM analysis of fracture surfaces in creep behaviour testing was performed to provide valuable information on the causes of fracture and surface changes, and to investigate the deformation of materials and specimen characteristics under prolonged loading at elevated temperatures. The surface SEM images of the fracture region of the creep tested specimens are presented in Fig. 6.

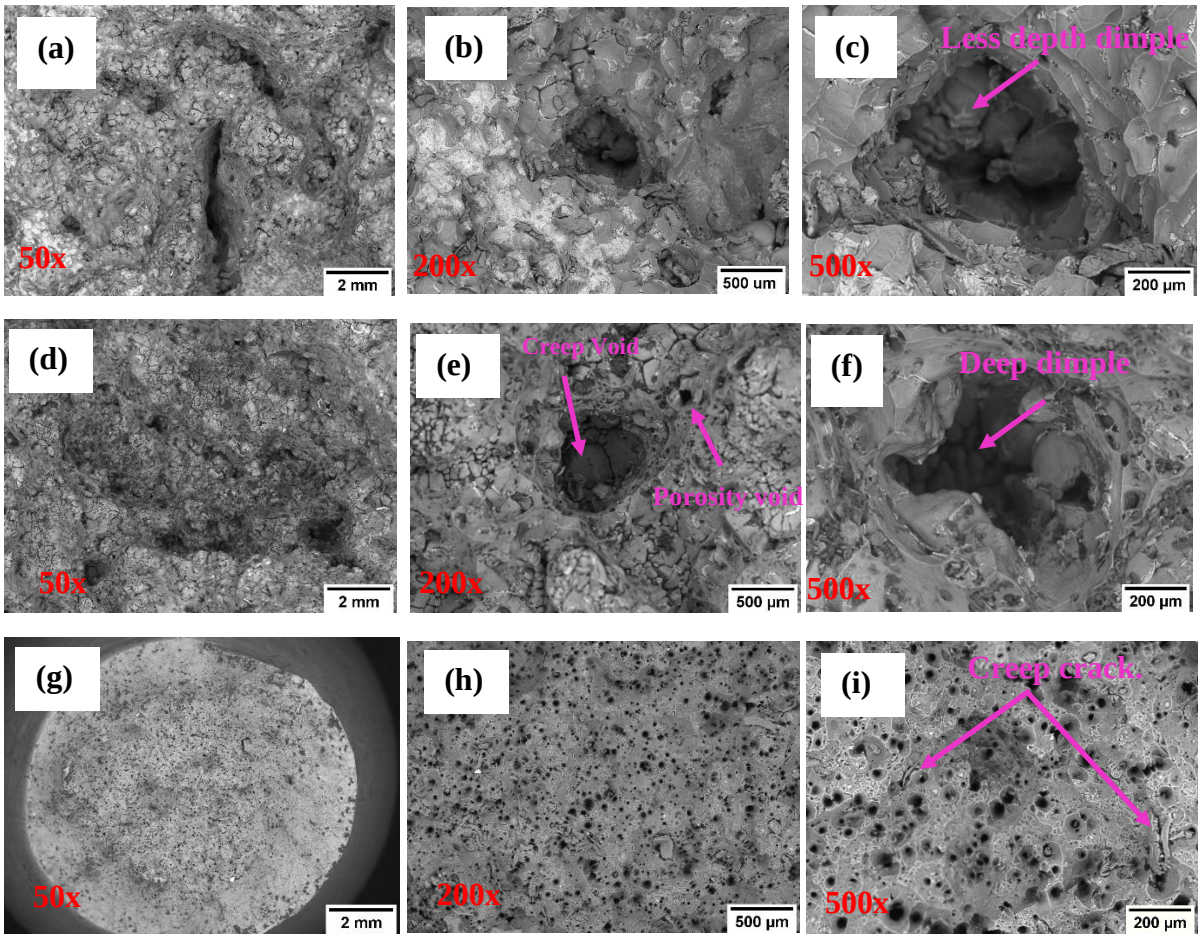

Fig. 6. SEM surface images of post-fracture test specimens were presented, first-row billet sample (50 MPa stress) with (a) 50 magnification, (b) 200 magnification, and (c) 500 magnification, second-row billet sample (70 MPa stress) with (d) 50 magnification, (e) 200 magnification, and (f) 500 magnification, third-row base material sample with (50 MPa stress) (g) 50 magnification, (h) 200 magnification, and (i) 500 magnification.

SEM images at varying magnifications of the samples subjected to tests at 50 MPa and 70 MPa stresses at a constant temperature of 250 °C were presented in the first and second rows. The third row displays SEM pictures of the original material under study at the same constant temperature and stress of 50 MPa. Images of aluminium 7075 alloy original sample and globular microstructure billet samples show their distinct deformation surface characteristics based on stress effects. The SEM study results reveal that the significant voids not observed in the original sample were observed in the billet sample due to gas porosity. Voids occurred during casting due to gas porosity, which is the result of gases trapped in the material matrix [27]. These voids appeared as oval cavity-like voids in SEM images. These significant voids revealed pits due to shrinkage during testing, and the pits coalesced leading to rapid rupture. A uniform diameter reduction was achieved by stress concentration in the original specimen, and a very small creep crack was observed before failure.

SEM surface images revealed that the material still maintained its overall integrity, even at elevated temperatures and low-stress conditions. Compared to the creep behaviour of billets produced in other semi-solid processing methods, grain shape and size emphasize the distribution of solid phases in the material and creep resistance, making holes less noticeable than in other methods [20]. At a stress level of 50 MPa, the SEM images show a smooth fracture surface with some evidence of small voids or pores. In the specimen obtained at 70 MPa stress, the pits of the fracture area were observed to be larger, and these pits may have formed due to high stress effects. However, the SEM images at higher stress (70 MPa) revealed a more complex fracture surface, and there was evidence of cracking and significant plastic deformation. It indicated that the material has a lower range of elasticity in response to increased stress [29]. At higher stress, the resistance to deformation decreases and thus increases the chance of fracture in a shorter period. [5,12]. Furthermore, it was found that there were weak points at the grain boundaries that caused crack initiation.

In the globular microstructure billet specimens, the holes and large defects caused by the casting process showed no significant traces of significantly affecting the corresponding creep behaviour. However, some voids were widely observed in the sample due to gas porosity. The particles observed in the original sample were tiny and well-networked, resulting in low dislocations. The development of creep voids that appeared due to high-stress concentrations in the original specimen combined with the ductile path resulted in ultimate failure [24]. In contrast, the particles observed in the billet sample were larger and less networked than the original sample, resulting in faster and easier dislocation due to the stress effect [30]. When stress is experienced at these particle-matrix interfaces and reaches a certain creep strain value, a creep void occurs due to interfacial failure. The macroscopic voids coalesce and form the creep voids quickly by connecting the microscopic voids. Aggregation of microscopic voids results in a crater-forming type of fracture with hemispherical dimples [31].

Furthermore, neck growth under compression in semi-solid alloy billets was delayed due to the inertia effect, which was consistent with the results of previous studies. A higher softening rate and deeper dimples were observed for the test specimen at higher stress than for the specimen tested at lower stress. These results observed that plasticity seems to be enhanced under high stress, which supports the earlier results of Mahathaninwong et al [20]. Structural defects such as porosity in billet specimens have acted as fracture initiation sites during testing. After initiation, the weak network of globular particles and coalescing of gas voids resulted in the formation of creep voids leading to failure, which supports the previous study results [32].

In this study, the strain exponent value of aluminium 7075 alloy globular microstructure billets was investigated. Also, Norton's law equation describes the relationship between the minimum creep rate of billets with globular microstructure and the applied creep stress at a constant temperature. **Fig. 7** presents the minimum creep rate versus the stress of a globular microstructure aluminium 7075 alloy billet at a constant temperature of 250 °C.

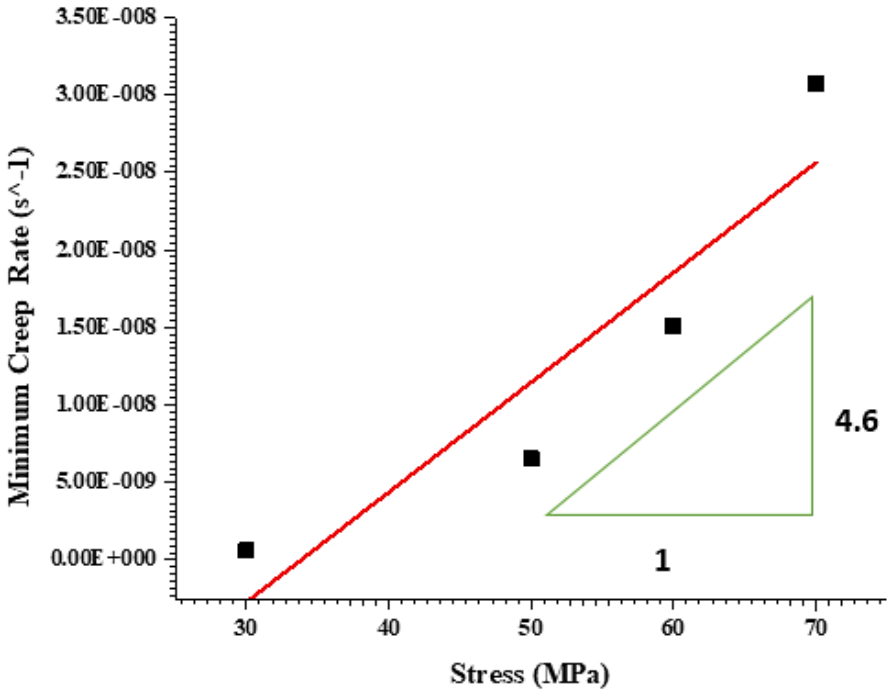

Fig. 7. Minimum creep rate versus the stress of globular microstructure aluminium 7075 alloy billet at a constant temperature of 250 °C.

The strain exponent value was found to be at n= 4.6 in the stress range of 30 to 70 MPa at a constant temperature of 250 °C. This is acceptable compared to previous study results [20,21,24]. It indicates the sensitivity of the material's strain response to time under creep conditions. It also helps to describe how the material deforms and how the strain changes over time. It describes the relationship between stress and strain of a globular structured billet undergoing plastic deformation. The value of "n" provides insights into how the material's strength changes during plastic deformation. A higher value of "n" indicates a higher rate of strain hardening, i.e. the

material becomes stronger at a faster rate as it deforms. This indicates that the material has reached a state of good plastic deformation. The strain exponent value provides valuable information about the creep resistance and overall mechanical properties of the material. According to Srivastava et al, at 350 °C and in the stress range of 1 to 5 MPa, the stress exponent for creep of this base material (aluminium 7075 alloy) was found to be near 1.3 [33]. Strain exponents of rheocast 7075-T6 and wrought 7075-T651 Al alloys at 300 °C and stress range of 20 to 60 MPa were found to be 5.9 and 7.9, respectively [24]. According to research by Mahathaninwong et al., the creep of semi-solid cast 7075-T Al alloy occurred with a stress exponent, n, of 6.3 at 200 °C and a stress range of 120 to 180 MPa [20]. An investigation of this strain exponent value will help guide new researchers on the development of globular structured billets. It helps to optimize manufacturing or processing conditions for materials, and to study the effects of microstructure, and the strain exponent can be used to achieve creep properties desired by manufacturers.

4. Conclusion

- A globular microstructure feedstock billet required for this experiment was produced using the DTM method. The average grain diameter, circularity, and aspect ratio of the primary phase particles of the prepared billet were 57.33 µm, 0.72, and 1.43, respectively, which is in good agreement with previous findings.

- The creep behaviour of globular microstructure feedstock billets used in semi-solid processing methods such as thixoforming was successfully studied at 250 °C under different stress conditions of 30 MPa, 50 MPa, 60 MPa, and 70 MPa. The creep behaviour of the globular microstructure billets responded better to stress effects.

- The globular microstructure billets showed reliable creep deformation at low-stress conditions of 30 MPa and 50 MPa, showing high resistance to creep at these conditions, and longer creep rupture time than the higher stress.

- The total creep strain of the billet specimen was lower than that of the non-billet original material specimen. However, globular microstructures promise to the higher creep strength in semi-solid process products because they show significant deformation with diffusion processes at constant strain rates and low stresses. Furthermore, the obtained values of this experiment provide insight into the effects and characteristics of the microstructure of aluminium 7075 alloys.

- The strain exponent value of globular structure billets was found to be n= 4.6 in the stress range of 30 to 70 MPa at a constant temperature of 250 °C. This determined 'n' value helps to control the dislocation slip and climb in creep deformation of globular microstructure feedstock billets.

5. Acknowledgement

Funding

The authors would like to thank the Ministry of Higher Education for providing financial support under Fundamental research grant No. FRGS/1/2019/TK03/UMP/02/8 University reference RDU1901122) and Universiti Malaysia Pahang Al-Sultan Abdullah for laboratory facilities as well as additional financial support under Internal Research grants RDU160311 and RDU603125.

Author contribution

Experiment work, data collection, and writing: A. Megalingam, supervision, and guidance: A.H. Ahmad and N.A. Alang, Data verification and moral support: J. Alias, and S. Naher.

Availability of data and material

Data availability Data will be made available on request.

Declarations

Ethics approval and consent to participate the manuscript has not been submitted to any other journal for simultaneous consideration. All authors voluntarily agreed to participate in this entire research study.

Consent for publication

The participants provided informed consent for the publication of their statements.

Competing interests

The authors declare that they have no known competing financial interests or personal relationships that could have appeared to influence the work reported in this paper.

6. Reference

1. W. Wang, P. Han, P. Peng, T. Zhang, Q. Liu, S. N. Yuan, L. Y. Huang, H. L. Yu, K. Qiao, and K. S. Wang, Friction Stir Processing of Magnesium Alloys: A Review, Acta Metall. Sin. (English Lett. **33**(1), 43–57 (2020).
2. E. Scharifi, R. Knoth, and U. Weidig, Thermo-mechanical forming procedure of high strength Aluminum sheet with improved mechanical properties and process efficiency, Procedia Manuf. **29**, 481–489 (2019).
3. T. Gao, L. Ying, P. Hu, X. Han, H. Rong, Y. Wu, and J. Sun, Investigation on mechanical behavior and plastic damage of AA7075 aluminum alloy by thermal small punch test: Experimental trials, numerical analysis, J. Manuf. Process. **50**(November 2019), 1–16 (2020).
4. L. G. Juganan, G. Govender, and A. F. Mulaba-Bafubiandi, Metallurgical and foundry parameters for the SSM forming of high strength aluminium-zinc-magnesium-copper (7075) alloy, Mater. Sci. Forum **618 619**, 611–614 (2009).
5. R. Molina, P. A. T. Aluminum, and M. R. Politecnico, Mechanical characterization of aluminium alloys for

high temperature applications Part 2: Al-Cu, Al-Mg alloys, Metall. Sci. Technol. **29**(1), 5–13 (2013).

6. A. T. Guner, D. Dispinar, and E. Tan, Microstructural and Mechanical Evolution of Semisolid 7075 Al Alloy Produced by SIMA Process at Various Heat Treatment Parameters, Arab. J. Sci. Eng. **44**(2), 1243–1253 (2019).

7. A. Megalingam, A. Hadi, B. Ahmad, M. Rashidi, B. Maarof, and K. Sudhakar, Viscosity measurements in semi - solid metal processing : current status and recent developments, Int. J. Adv. Manuf. Technol. (0123456789), (2021).

8. S. Nafisi and R. Ghomashchi, Impact of melt treatment on semi-solid metal processing, J. Alloys Compd. **436**(1–2), 86–90 (2007).

9. Rogal, J. Dutkiewicz, L. Lityńska-Dobrzańska, B. Olszowska-Sobieraj, and M. Modigell, Positive effect of Sc and Zr on globular microstructure formation in AA7075 thixoforming feedstock, AIP Conf. Proc. **1353**, 1039–1044 (2011).

10. C. T. W. Proni, M. H. Robert, and E. J. Zoqui, Effect of casting procedures in the structure and flow behaviour of semisolid A356 alloy, Arch. Mater. Sci. Eng. **73**(2), 82–93 (2015).

11. A. Megalingam, A. H. Ahmad, N. A. Alang, J. Alias, and N. A. A. Razak, Application of Response Surface Methodology for Parameter Optimization of Aluminum 7075 Thixoforming Feedstock Billet Production, J. Mater. Eng. Perform. (Ref 11), (2022).

12. W. S. Lee, W. C. Sue, C. F. Lin, and C. J. Wu, Strain rate and temperature dependence of the dynamic impact properties of 7075 aluminum alloy, J. Mater. Process. Technol. **100**(1), 116–122 (2000).

13. K. P. Sołek, Ł. Rogal, and P. Kapranos, Evolution of Globular Microstructure and Rheological Properties of Stellite^{TM} 21 Alloy after Heating to Semisolid State, J. Mater. Eng. Perform. **26**(1), 115–123 (2017).

14. S. Kumar, S. Ramteke, S. Chelika, and C. Vanitha, Creep behavior of Al-Si-Mg alloy by hot impression creep test, Mater. Today Proc. **41**, 1207–1211 (2019).

15. P. Zhao, J. Shen, and H. Zhang, Short-term creep behavior in P91 heat-resistant steel at low stress, Mater. Sci. Forum **850**, 922–926 (2016).

16. S. P. Shivakumar, A. S. Sharan, and K. Sadashivappa, Constitutive modeling of creep properties of Aluminum 6061 Alloy, IOP Conf. Ser. Mater. Sci. Eng. **310**(1), (2018).

17. S. Masoud, R. Mahmudi, and A. Reza, A comparative study on the effects of Gd , Y and La rare-earth elements on the microstructure and creep behavior of AZ81 Mg alloy Materials Science & Engineering A A comparative study on the effects of Gd , Y and La rare-earth elements on the microstructu, Mater. Sci. Eng. A **790**(October), 139712 (2020).

18. J. Chen, H. Fujii, Y. Sun, Y. Morisada, and K. Kondoh, Effect of grain size on the microstructure and mechanical properties of friction stir welded non-combustive magnesium alloys, Mater. Sci. Eng. A **549**, 176–184 (2012).

19. L. T. Li, Y. C. Lin, H. M. Zhou, and Y. Q. Jiang, Modeling the high-temperature creep behaviors of 7075 and 2124 aluminum alloys by continuum damage mechanics model, Comput. Mater. Sci. **73**(2013), 72–78 (2013).

20. N. Mahathaninwong, Y. Zhou, S. E. Babcock, T. Plookphol, J. Wannasin, and S. Wisutmethangoon, Creep rupture behavior of semi-solid cast 7075-T6 Al alloy, Mater. Sci. Eng. A **556**, 107–113 (2012).

21. V. Srivastava, J. P. Williams, K. R. McNee, G. W. Greenwood, and H. Jones, Low stress creep behaviour of 7075 high strength aluminium alloy, Mater. Sci. Eng. A **382**(1–2), 50–56 (2004).

22. Y. C. Lin, X. Bin Peng, Y. Q. Jiang, and C. J. Shuai, Effects of creep-aging parameters on aging precipitates of a two-stage creep-aged Al–Zn–Mg–Cu alloy under the extra compressive stress, J. Alloys Compd. **743**, 448–455 (2018).

23. Y. C. Lin, Y. Q. Jiang, H. M. Zhou, and G. Liu, A New Creep Constitutive Model for 7075 Aluminum Alloy Under Elevated Temperatures, J. Mater. Eng. Perform. **23**(12), 4350–4357 (2014).

24. S. Thongkam, S. Wisutmethangoon, J. Wannasin, S. Chantaramanee, and T. Plookphol, Creep of rheocast 7075 aluminum alloy at 300 °C, Appl. Mech. Mater. **372**, 288–291 (2013).

25. A. H. Ahmad, S. Naher, and D. Brabazon, Direct thermal method of aluminium 7075, Adv. Mater. Res. **939**, 400–408 (2014).

26. I. U. Ferdous, N. A. Alang, J. Alias, A. H. Ahmad, and S. Mohd Nadzir, Rupture Life and Failure Mechanism of Grade 91 Steel Under the Influence of Notch Constraint, J. Fail. Anal. Prev. **23**(2), 497–510 (2023).

27. C. Ahn, I. Jo, C. Ji, S. Cho, B. Mishra, and E. Lee, Creep behavior of high-pressure die-cast AlSi10MnMg aluminum alloy, Mater. Charact. **167**(May), 110495 (2020).

28. A. Ghosh and M. Ghosh, Microstructure and texture development of 7075 alloy during homogenisation, Philos. Mag. **98**(16), 1470–1490 (2018).

29. S. W. Chen and C. C. Huang, Solidification curves of Al-Cu, Al-Mg and Al-Cu-Mg alloys, Acta Mater. **44**(5), 1955–1965 (1996).

30. A. V. Mikhaylovskaya, O. A. Yakovtseva, I. S. Golovin, A. V. Pozdniakov, and V. K. Portnoy, Superplastic deformation mechanisms in fine-grained Al-Mg based alloys, Mater. Sci. Eng. A **627**, 31–41 (2015).

31. S. Mohan Kumar, R. Pramod, M. E. Shashi Kumar, and H. K. Govindaraju, Evaluation of fracture toughness and mechanical properties of aluminum alloy 7075, T6 with nickel coating, Procedia Eng. **97**, 178–185 (2014).

32. A. Ulbricht, L. A. Ávila Calderón, K. Sommer, G. Mohr, A. Evans, B. Skrotzki, and G. Bruno, Evolution of Creep Damage of 316L Produced by Laser Powder Bed Fusion, Adv. Eng. Mater. **25**(12), (2023).

33. N. Srivastava and M. A. Burns, Analysis of non-Newtonian liquids using a microfluidic capillary viscometer, Anal. Chem. **78**(5), 1690–1696 (2006).